

# Hidden chaotic sets in a Hopfield neural system

Marius-F. Danca\*

Department of Mathematics and Computer Science,  
Avram Iancu University,  
400380 Cluj-Napoca, Romania,  
and  
Romanian Institute of Science and Technology,  
400487 Cluj-Napoca, Romania  
Email: danca@rist.ro

Nikolay Kuznetsov

Department of Applied Cybernetics,  
Saint-Petersburg State University, Russia  
and  
Department of Mathematical Information Technology,  
University of Jyväskylä, Finland  
email: nkuznetsov239@gmail.com

March 13, 2021

## Abstract

In this paper we unveil the existence of hidden chaotic sets in a simplified Hopfield neural network with three neurons. It is shown that beside two stable cycles, the system presents hidden chaotic attractors and also hidden chaotic transients which, after a relatively long life-time, fall into regular motions along the stable cycles.

**keyword** Hopfield neural network; Hidden chaotic attractor; Hidden chaotic transient; Limit cycle

## 1 Introduction

The origin of transient chaos is well known: it is due to nonattracting chaotic saddles in phase space [1–7]. Transient chaos is a common phenomenon of many engineering, physical and

---

\*Corresponding author

biological systems. Compared with chaos, which is characterized as a long-term behavior, the transient chaos, is a phenomenon which appears when a nonlinear system behaves chaotically during some transient time interval and the trajectories in a certain region of phase space behave chaotically for a while, after which falls into a regular motion. These systems may initially exhibit an aperiodic behavior and sensitivity to initial conditions (i.e. “chaos”) and after a period of time, it settles down on a periodic orbit or fixed point.

Such phenomena were observed in radio circuits [8], hydrodynamics [9], neural networks [10], standard models of nonlinear systems such as Rössler system [11], Lorenz system [4,12], experiments (e.g. synchronization of two unidirectionally coupled Chua circuits [8]), maps [13], species extinction [14] and so on.

In some applications, the transient chaos can be quite disastrous, as in situations of voltage collapse or species extinction. Therefore it is often desirable to sustain transient chaos. Thus, conversion of the transient chaos into sustained chaos can avoid catastrophes related to sudden chaos collapses, even in the absence of external perturbations (i.e. chaos anticontrol) [5, 15]. On the other side, in some situations, the chaotic transients are highly undesirable, so that control techniques are useful (see e.g. the control method known as “partial control” [16]).

In a recent paper [17] a new phenomenon of transient chaos, *doubly transient chaos*, fundamentally different from the hyperbolic and nonhyperbolic transient chaos reported in the existing literature is revealed. This type of phenomenon appears in many systems (chemical reactions, binary star behavior, etc.) and it is likely far less predictable than has been previously thought.

A Neural Network (NN) is a mathematical or computational model inspired by biological neural networks that consists of interconnected groups of neurons. Without chaotic behavior neural systems cannot be adequately addressed and fully understood [18]. Neurobiological chaos, omnipresent in the brain, points out several possible approaches of understanding how the brain works and this is demonstrably so, in the somatosensory and the olfactory cortices [19]. Many NNs, such as discrete time NNs, or continuous (time-delayed) NNs, may behave chaotically. The roles of chaos in this type of systems have been investigated in many papers in the last years [20–25].

Hopfield Neural Networks (HNN) are constructed from artificial neurons and represent particular cases of NNs inspired by spin systems [26]. Even if it is not easy to be discovered, chaos and hyperchaos have been identified in many HNNs [10, 27–33].

From the computational perspective point of view, based on the connection of their basins of attraction with equilibria in the phase space, it is natural to suggest the following attractors classification

**Definition 1.** [34–38] *An attractor is called a self-excited attractor if its basin of attraction intersects with any open neighborhood of an equilibrium; otherwise, it is called a hidden attractor.*

*Self-excited attractors* can be visualized numerically by a standard computational procedure, in which after a transient process, a trajectory starting from a point of a neighborhood of unstable equilibrium is attracted to the attractor, while the basin of attraction for a hidden attractor is not connected with any equilibrium. Therefore, for the numerical localization of hidden attractors it is necessary to develop special analytical-numerical procedures [34,37,39].

Hidden attractors can appear in systems with no-equilibria or in multistable systems with only stable equilibrium. Coexisting self-excited attractors in multistable systems can be found using a standard computational procedure, whereas there is no regular way to predict the existence or coexistence of hidden attractors in a system (for various examples of multistable engineering systems refer to [38, 40]).

To verify numerically that a chaotic attractor is hidden, one has to check that all trajectories starting in small neighborhoods of unstable equilibria, are not attracted by the attractor (see e.g. [35, 37]).

In this paper we consider the case of a 3-neuron simplified HNN and we unveil, beside two stable cycles, its hidden chaotic attractors and hidden chaotic transients.

## 2 The simplified Hopfield neural network

The 3-neuron HNN considered in this paper, is a simplified variant of the simplest example of a system that “realizes everything”<sup>1</sup> and has “maximal dynamic complexity” [42], is modeled by the following ODEs [10]

$$\dot{x}_i = -x_i + \sum_{j=1}^3 w_{ij} f(x_j), \quad i = 1, 2, 3, \quad (1)$$

with  $f(x_j) = \tanh(x_j)$  and with the weight matrix

$$W = \begin{bmatrix} w_{11} & w_{12} & w_{13} \\ w_{21} & w_{22} & w_{23} \\ w_{31} & w_{32} & w_{33} \end{bmatrix} = \begin{bmatrix} 2 & -1.2 & 0 \\ 1.9995 & 1.71 & 1.15 \\ -4.75 & 0 & 1.1 \end{bmatrix}.$$

and whose topological connection is presented in Fig. 1.

We show numerically that, beside two stable cycles and hidden chaotic attractors, the HNN (1) admits a new type of coexisting hidden sets: *hidden chaotic transients*<sup>2</sup>.

With the above values of weights, the system (1) reads

$$\begin{aligned} \dot{x}_1 &= -x_1 + 2 \tanh(x_1) - 1.2 \tanh(x_2), \\ \dot{x}_2 &= -x_2 + 1.9995 \tanh(x_1) + 1.71 \tanh(x_2) + 1.15 \tanh(x_3), \\ \dot{x}_3 &= -x_3 - 4.75 \tanh(x_1) + 1.1 \tanh(x_3). \end{aligned} \quad (2)$$

The sigmoid-like function  $\tanh(x)$ , is used to approximate the switch discontinuity in  $x = 0$ , typically to neurons dynamics.

The HNN system (2) is symmetrical with respect to the origin and has the following equilibria

$$X_0^* = (0, 0, 0), \quad X_{1,2}^* = \pm(0.493, 0.366, -3.267).$$

---

<sup>1</sup>In other words, its dynamics can be determined with an arbitrary accuracy using the parameters on which it depends [41].

<sup>2</sup>Transient dynamics of hidden attractors in a 4D system are analyzed in [43].

The Jacobian is

$$J = \begin{bmatrix} 1 - 2 \tanh^2(x_1) & -1.2 + 1.2 \tanh^2(x_2) & 0 \\ 1.9995 - 1.9995 \tanh^2(x_1) & 0.71 - 1.71 \tanh^2(x_2) & 1.15 - 1.15 \tanh^2(x_3) \\ -4.75 + 4.75 \tanh^2(x_1) & 0 & 0.1 - 1.1 \tanh^2(x_3) \end{bmatrix},$$

and the eigenvalues of  $X_0^*$  are  $\lambda_1 = 1.942$  and  $\lambda_{2,3} = -0.066 \pm 1.879i$  while the eigenvalues of  $X_{1,2}^*$  are  $\lambda_1 = -0.987$  and  $\lambda_{2,3} = 0.538 \pm 1.286i$ . Therefore, equilibria are unstable: one attracting focus saddle,  $X_0^*$ , and two repelling focus saddles  $X_{1,2}^*$  (ingredients of transients chaos).

### 3 Hidden chaotic transients of the Hopfield neural network

The numerical integration of the HNN (2) is realized with the Matlab differential solver *ode45* with option *opts = odeset('RelTol', 1e - 9, 'AbsTol', 1e - 9)* which yields 8 decimals accurate results<sup>3</sup>.

In Hopfield like systems it is common to find transients, which are interpreted as being chaotic (see e.g. [10]). Generally, the duration of these transients is rather short before they settle down on some periodic stable attractor [6] (in [46] the life-time of hidden chaotic transient sets of the Rabinovich-Fabrikant system is of order of 160).

We show that, for the considered system, beside hidden chaotic attractors, there are pairs of coexisting relative long chaotic transients with life-time  $[0, T^*]$ ,  $T^* > 1000$ , which, following Definition 1, can be considered as hidden. Also, there are short transients to two stable cycles which, due to their short life-time (with generally  $T^* < 500 - 700$ ), cannot be considered chaotic in the usual sense.

The system admits two stable cycles, denoted  $C_1$  and  $C_2$  (Fig. 2 (a), red and blue plots respectively). These cycles can be reached, either via two coexisting transient chaotic trajectories  $H_{1,2}$  starting from initial points situated far from equilibria, e.g. the points  $\pm(1.9, 3, 1)$  considered in this work (the light red and light blue phase plots in Fig. 2 (a), and time series plots in Fig. 2 (b)-(d)), or by starting from small  $\delta$ -vicinity (with  $\delta = 1.5E-4$ ) of unstable equilibria  $X_{0,1,2}^*$  (see Fig. 3, where the case of  $C_2$  is considered, with the initial condition  $(-0.49, -0.36, 3.26)$  belonging to a small neighborhood of  $X_2^*$ . The case of  $C_1$  can be treated similarly). While in the case of the chaotic transients,  $H_{1,2}$ , starting relatively far to equilibria (points  $\pm(1.9, 3, 1)$ ), a large transient life-time  $[0, T^*]$ , with  $T^* = 1000$  (Fig. 2 (b)-(d)), is necessary to reach  $C_{1,2}$ , for the trajectories starting from  $\delta$ -vicinity of  $X_{0,1,2}^*$ , the transients are extremely short, about 1/10 of the life-time of the chaotic transients  $H_{1,2}$  (Fig. 3). Therefore, in this paper, the chaotic transients are the chaotic trajectories with life-time  $T^* > 1000$ .

In the spirit of Definition 1, one have to verify that, after very short transients, all trajectories starting from small neighborhoods of unstable equilibria must be attracted by

---

<sup>3</sup>Matlab implicitly uses default values  $RelTol = .001$  and  $AbsTol = .000001$  and the approximate error at each step  $e_k$  is ensured to be  $e_k \leq \max(RelTol \times x_k, AbsTol)$ , for all  $k$ , where  $x_k$  is the value calculated at the node  $t_k$  (see e.g. [44] for the used Runge-Kutta and other numerical methods utilized by Matlab). In [45] it is suggested  $RelTol = 10^{-(m+1)}$  for  $m$  precise digits of the required solution.

the stable cycles  $C_{1,2}$  and not by the chaotic transients  $H_{1,2}$ . While trajectories starting from neighborhoods of e.g.  $X_0^*$  tends either to  $C_1$  or  $C_2$ , because  $X_0^*$  belongs to the separatrix of the basins of attractions of  $C_1$  and  $C_2$  (See Fig. 4 (a), where for clarity, only 50 trajectories are considered), the trajectories starting from neighborhoods of  $X_1^*$  and  $X_2^*$  tends to  $C_1$  and  $C_2$  respectively (see Fig. 4 (b) for the case of  $X_2^*$ ).

**Remark 2.** *By improving the numerical approximations (smaller values for  $RelTol$  and  $AbsTol$ ), it is possible to obtain longer hidden chaotic transients. However, related to the length of the integration interval, precautions should be considered, since a too large time interval could lead to inaccurate numerical solutions (see e.g. [47] for the case of Lorenz system). Moreover, there seems to be a time scale scale in all natural processes beyond which structural stability and calculability become incompatible [48].*

The shape of the trajectories starting within  $V_{X_0^*}$  and  $V_{X_{1,2}^*}$  are consistent with the equilibria type: the trajectories from vicinities  $V_{X_{1,2}^*}$  exit by scrolling equilibria  $X_{1,2}$  in the unstable two-dimensional manifold (Fig. 4 (b)), while the trajectories from the vicinity of  $X_0^*$  leave  $V_{X_0^*}$  along the one-dimensional unstable manifold of  $X_0^*$  (Fig. 4 (a)).

Since  $H_{1,2}$  can be obtained only from attraction basins situated relatively far from the equilibria, and trajectories starting from equilibria neighborhoods tend almost directly to the stable cycles, we can consider the chaotic transients  $H_{1,2}$  as being hidden and  $C_{1,2}$  self-excited stable limit cycles. Fig. 5, where a  $\delta$ -vicinity of order of  $10^{-4}$  is considered, shows that there exists regions of  $H_{1,2}$  containing initial points wherefrom almost all trajectories reach  $H_{1,2}$ . Time series of the state variable  $x_1$  for the considered trajectories (Fig. 6), reveal initial points generating hidden chaotic trajectories with long life-time ( $T^* > 1000$ ) which can be considered hidden chaotic transients, but also short transients.

For the numerical localization of hidden attractors, a special analytical-numerical procedure can be found in e.g. [37]. In this paper, for transient hidden sets the following initial conditions have been found:  $\pm(1.9, 3, 1)$ . The basin of attraction of the chaotic hidden transient  $H_1$  determined in the plane  $x_3 = 1$  is presented in Fig. 7 (a). As can be seen, the initial conditions generating the transient hidden sets (green) are disposed in small shapes located along oblique strips and form fractal clusters. The remaining area (red) represents the initial conditions which lead to the stable cycle  $C_1$ . The zoom of the 1/100 reduced rectangular region centered in  $(1.9, 3)$  in Fig. 7 (b), reveals the selfsimilarity property: any zoomed region containing initial conditions, reveals new and new initial conditions for hidden transients.

Note that the coexistence of the hidden chaotic transients  $H_{1,2}$  and the stable cycles  $C_{1,2}$ , are ensured by the entrainment of limit cycles by chaos (see [49], where the replication of sensitivity and the existence of infinitely many unstable periodic solutions were rigorously proved and [50], where this result is applied in Hopfield systems). Based on this result, the transient hidden chaotic sets  $H_{1,2}$  differ from the short transients to  $C_{1,2}$  starting from equilibria neighborhoods.

The following approach is based on the analysis of structural stability introduced by Andronov and Pontryagin in 1937, which quantifies how the system responds to changes of the parameters. As known, a flow pattern is qualified as structural stable if small variations of a parameter do not affect the flow structure in a topological sense. In other words, for small parameter variations, the new flow is topologically equivalent with the non-perturbed flow (see e.g. [51, 52]). The results are summarized in the Fig. 8 where  $w^*$  are the values

of the matrix  $W$ . The set of initial parameters data is perturbed around  $w^*$ . Thus, every parameter  $w_{ij}$  is perturbed, while the rest of the parameters are fixed. With perturbations of order  $10^{-5}$ , the system changes its dynamics. Thus, for  $w_{11}, w_{22}, w_{31} < \tilde{w}_1^*$ , where  $\tilde{w}_1^*$  is a point situated at a small distance of about  $10^{-4}$  from  $w^*$ , the system evolves chaotically (Fig. 8 (a)). Because the chaotic trajectory seem to last for extremely long life-time (even for  $T > 50000$ ), the underlying chaotic set can be considered a chaotic attractor (see e.g. the time series for the component  $x_1$  and the phase plot for  $w_{11} = 1.995$ ; for image clarity, only  $T = 5000$  has been considered). Moreover, due to the modality in which these attractors have been obtained and due to their characteristics, they are hidden (not self-excited). For  $\tilde{w}_1^* < w_{11}, w_{22}, w_{31} < w^*$  the system presents hidden chaotic transients (see Fig. 8 (a)  $w_{11} = 1.9995$ ), while for  $w_{11}, w_{22}, w_{31} > w^*$  the system pulls the trajectories along the stable cycles (Fig. 8 (a)  $w_{11} = 2.05$ ).

Reversely, while  $w_{12}, w_{21}, w_{23}, w_{33}$  increase their values, the system dynamics change from regular motions (stable cycles  $C_{1,2}$ ) to hidden chaotic transients (Fig. 8 (b)). Again, there exists values of  $w_{12}, w_{21}, w_{23}, w_{33}$ , denoted by  $\tilde{w}_2^*$ , such that for  $w_{12}, w_{21}, w_{23}, w_{33} > \tilde{w}_2^*$ , the system evolves along a hidden chaotic attractor.

Because the parameter perturbations, small compared with the attractors size, put the system into one of other permissible states, one can consider that the system is unstable structural.

## 4 Conclusion

In this paper, following intensive numerical tests, we shown and verified numerically with 8 accurate decimals results, that for the considered parameters value, the HNN (1) presents hidden transient chaotic sets  $H_{1,2}$  which last for a life-time  $T^* > 1000$ , while for slightly modified parameters value, the system changes dynamics and presents either hidden chaotic attractors or stable cycles. The chaotic transients have a relative long life-time with fractal attraction basins. Their shape of the hidden chaotic transients seems to be deformed by the form of the coexisting limit cycles and unstable equilibria. Therefore,  $H_1$  and  $H_2$  have a complex structure. So, one may say that the behavior is rather natural here. Since chaotic behavior in neural activity seems to be unavoidable, chaos control and anticontrol of these transient hidden chaotic sets are an unexplored theme yet and they offer an exciting subject for a future research. On the other side, as known, data is often of dubious quality (noisy and incomplete). It is a matter of fact that noise have a serious impact on real biological systems. Therefore, a future study of the role of noisy networks [53–55] in dynamics of transient chaos for the considered HNN would be of interest.

**Acknowledgment.** M.F. Danca is supported by Tehnic B SRL. M.F. Danca and N. Kuznetsov thank Russian Science Foundation (project 14-21-00041). The authors appreciate the valuable suggestion given by reviewers and also thank Vlad-Marius Gruitu of University of Manchester, who helped to determine the attraction basin.

## References

- [1] Grebogi C, Ott E, Yorke JA. Phys Rev Lett 1983;50:935.
- [2] Kantz H, Grassberger P. Phys D 1985;17:75.
- [3] Kaplan JL, Yorke JA. Commun Math Phys 1979;67:93.
- [4] Yorke JA, Yorke ED. J Stat Phys 1979;21:263.
- [5] Shulenburger L, Lai Y-C, Yalçinkaya T, Holt RD. Phys Lett A 1999;260:156.
- [6] Nusse HE, Yorke JA. Phys D 1989;36:137.
- [7] Hsu GH, Ott E, Grebogi C. Phys Lett A 1988;127:199.
- [8] Zhu L, Raghun A, Lai YC. Phys Rev Lett 2001;86:4017.
- [9] Ahlers G, Walden RW. Phys Rev Lett 1980;44:445.
- [10] Yang XS, Yuan, Q. Neurocomputing 2005;69:232.
- [11] Dhamala M, Lai YC, Kostelich EJ. Phys Rev E 2000;61:6485.
- [12] Vadasz P. App Math Lett 2010;23:503.
- [13] Astafev GB, Koronovskii AA, Khramov AE. Tech Phys Lett+ 2003;2:923.
- [14] McCann K, Yodzis P. Am Nat 1994;144:873.
- [15] Dhamala M, Lai YC. Phys Rev E 1999;59:1646.
- [16] Capeáns R, Sabuco J, Sanjuán MAF, Yorke, JA. Philos Tr Soc A 2017.
- [17] Motter AE, Gruiz M, Károlyi G, Tél T. Phys Rev Lett 2013;111:194101.
- [18] Skarda CA, Freeman WJ. Behavioral and Brain Sciences 1987;10:161.
- [19] Freeman WJ. Neurodynamics: An exploration in mesoscopic brain dynamics. Springer; 2000.
- [20] Dror G, Tsodyks M. Neurocomputing 2000;32:365-370.
- [21] Nara S, Davis P, Kawachi M, Totsuji H. Int J Bifurcat Chaos 1995;5:1205.
- [22] Cao J, Lu J. Chaos 2006;16:013133.
- [23] Aihara K, Takebe T, Toyoda M. Phys Lett A 1990;144:333.
- [24] Freeman WJ. Int J Bifurcat Chaos 1992;2:451.
- [25] Guckenheimer J, Oliva RA. SIAM J Appl Dyn Syst 2002;1:105.

- [26] Kawamura M, Okada M. *J. Phys. A-Math. Gen.* 2002;35:253.
- [27] Xu C, Li, P. *Chaos Soliton Fract* 2017;96:139.
- [28] Hopfield JJ. *Proc Nat Acad Sci USA* 1982;79:2554.
- [29] Kaslik E, Balint S. *Chaos Soliton Fract* 2006; doi:10.1016/j.chaos.2006.03.107, 2006
- [30] Huang C, Huang L, Feng, J, Nai M, He Y. *Chaos Soliton Fract* 2007;34:795.
- [31] Yang XS, Huang Y. *Chaos* 2006;16:033114.
- [32] Huang WZ, Huang Y. *App Mat Comput* 2008;206:1.
- [33] Park MJ, Kwon OM, Park Ju H, Lee SM, Cha EJ. *Chinese Phys B* 2011;20:110504.
- [34] Leonov GA, Kuznetsov NV. *Int J Bifurcat Chaos* 2013;23:1330002.
- [35] Leonov G, Kuznetsov N, Mokaev T. *Eur Phys J-Spec Top* 2015;224:1421.
- [36] Leonov GA. Kuznetsov NV, Vagaitsev VI. *Phys Lett A* 2011;375:2230.
- [37] Leonov GA, Kuznetsov NV, Vagaitsev VI. *Phys D* 2012;241:1482.
- [38] Kuznetsov NV. (2016). Hidden attractors in fundamental problems and engineering models. A short survey, AETA 2015: Recent Advances in Electrical Engineering and Related Sciences. *Lecture Notes in Electrical Engineering*, 371, 13.
- [39] Dudkowski D, Jafari S, Kapitaniak T, Kuznetsov NV, Leonov GA, Prasad A. *Phys Rep* 2016;637:1.
- [40] Pisarchik A, Feudel U. *Phys Rep* 2014;540:167.
- [41] Abramyan AK, Vakulenko SA. *Theor Math Phys+* 2002;130:245.
- [42] Vakulenko SA. *Adv Diff Equat* 2000;5:1739.
- [43] Dang XYD, Li CB, Bao BC, Wu HG. *Chinese Phys B* 2015;24:050503.
- [44] Shampine LF, Gladwell I, Thompson S. *Solving ODEs with MATLAB*. Cambridge Univ. Press; 2003.
- [45] Brenan KE, Campbell SL, Petzold LR. *Numerical Solution of Initial-Value Problems in Differential-Algebraic Equations (SIAM Classics in Applied Mathematics, 14)*. SIAM: Philadelphia; 1996.
- [46] Danca MF. *Nonlinear Dynam* 2016;86:1263.
- [47] Kehlet B, Logg A. Quantifying the computability of the Lorenz system. arXiv:1306.2782v1 [math.NA] 12 Jun 2013 <http://arxiv.org/abs/1306.2782>
- [48] Thom R. *Dialectica* 1975;29:71.

- [49] Akhmet MU, Fen, MO. *J Nonlinear Sci* 2014;24:411.
- [50] Akhmet M, Fen MO. *Neurocomputing* 2014;145:230.
- [51] Anosov D, Arnold V. *Dynamical Systems I*, Springer, New York, 1985.
- [52] Arnold V. *Mathematical Methods of Classical Mechanics*, Springer, New York, 1978.
- [53] Ushakov Yu V, Dubkov AA, Spagnolo B. *Phys Rev Lett* 2011;107:108103.
- [54] Pankratova EV, Polovinkin AV, Bernardo S. *Phys Lett A* 2005;344:43-50.
- [55] Augello G, Spagnolo B. *Eur Phys J B* 2008;65:443.
- [56] Chaudhuri U, Prasad A. *Phys Lett A* 2014;378:713.

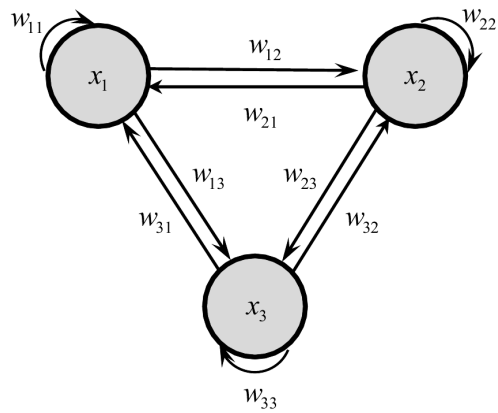


Figure 1: Topological connection.

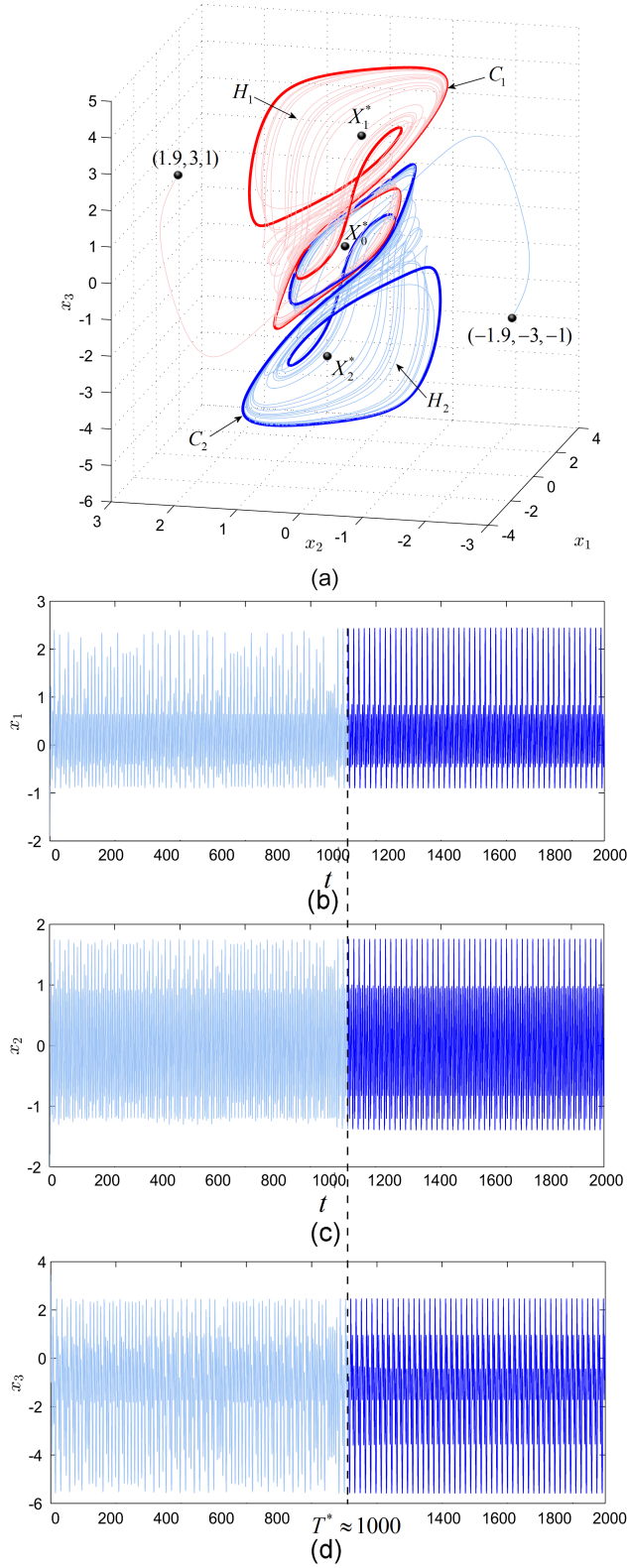


Figure 2: Hidden chaotic transients  $H_1$  (light red plot) and  $H_2$  (light blue plot) of the HNN (2) obtained with initial conditions  $\pm(1.9, 3, 1)$  and stable cycles  $C_1$  and  $C_2$  (red plotted and blue plot respectively). (a) Phase plots; (b)-(d) Time series for initial condition  $(-1.9, -3, -1)$  revealing the hidden chaotic transient  $H_2$  and the stable cycle  $C_2$ .

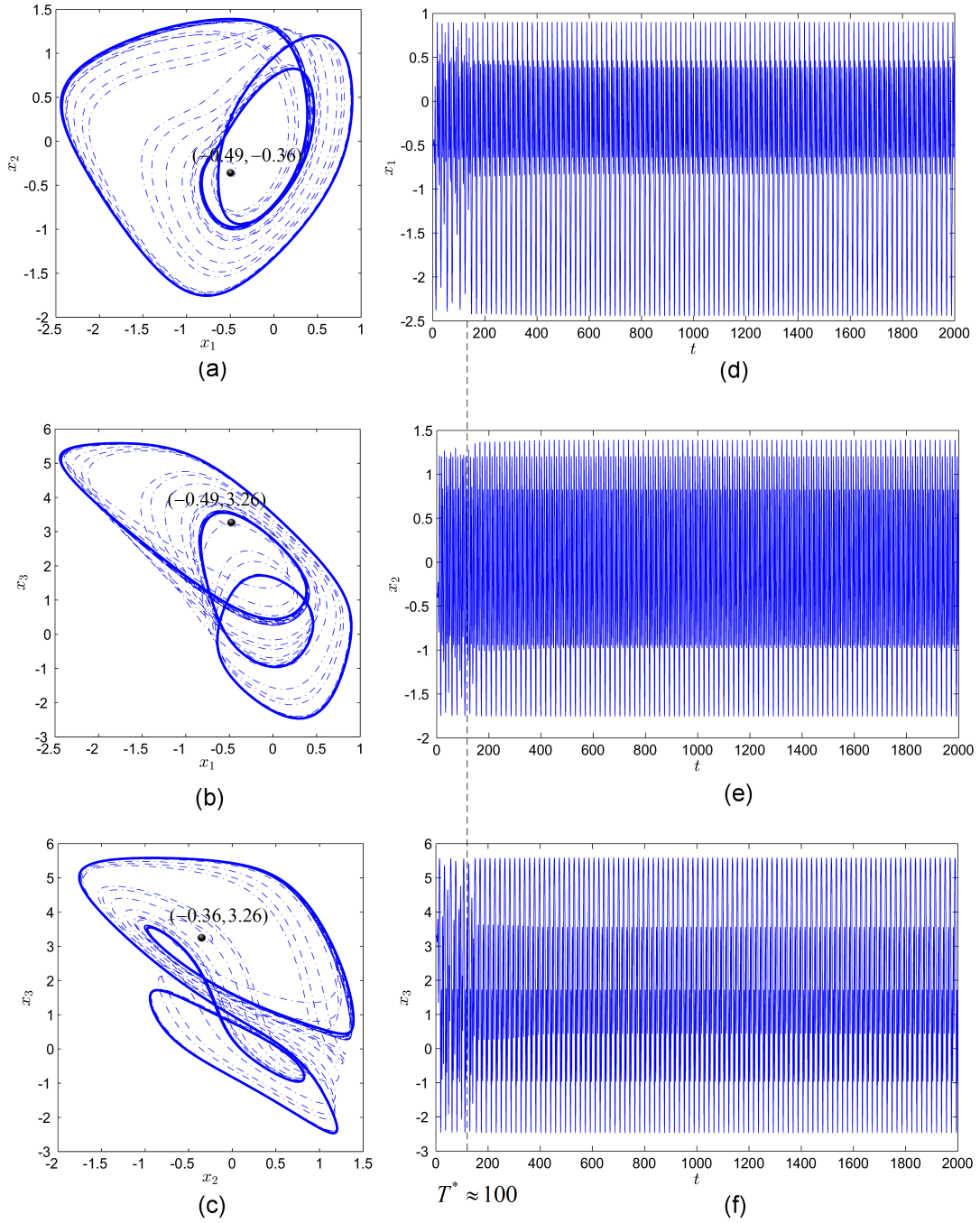


Figure 3: Stable cycle  $C_2$  obtained after a short transient ( $T^* \approx 100$ ) starting from the neighborhood of  $X_2^*$  (point  $(-0.49, -0.36, 3.26)$ ). (a)-(c) Phase plane plots. Transients to  $C_2$  are dotted lined; (d)-(f) Time series.

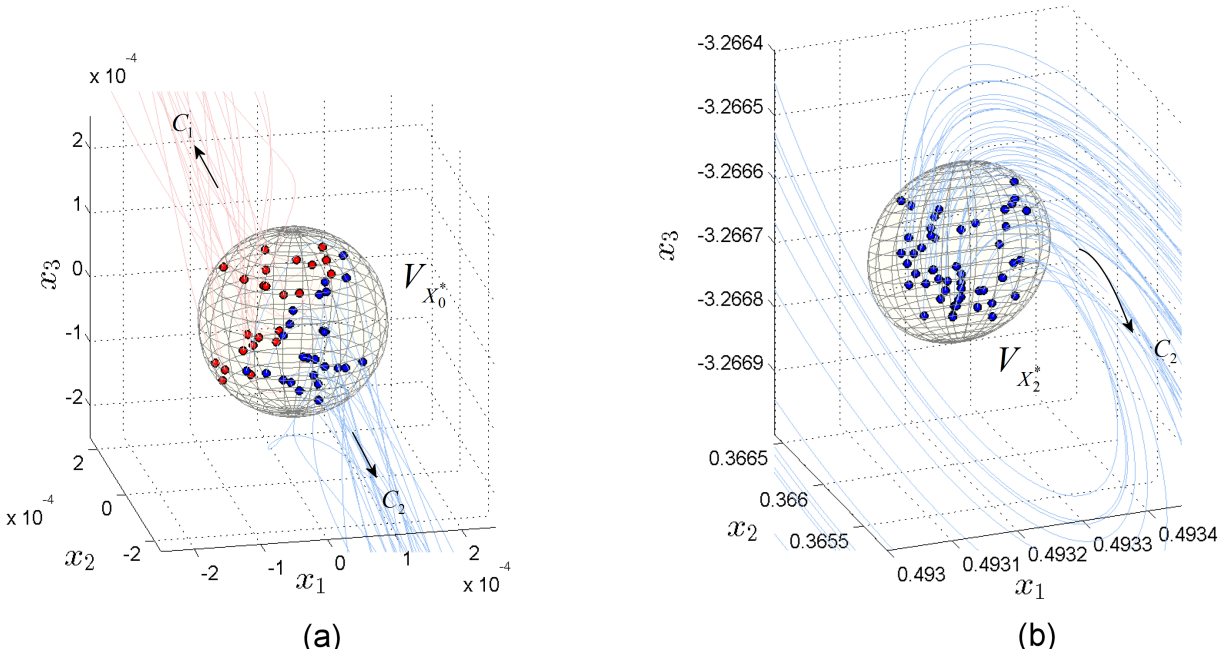


Figure 4: 50 trajectories starting from neighborhoods  $V_{X_0^*}$  and  $V_{X_2^*}$  of equilibria  $X_0^*$  and  $X_2^*$ . a) Trajectories from  $V_{X_0^*}$  tend either to  $C_1$  (light red), or to  $C_2$  (light blue); b) All the considered 50 trajectories from  $V_{X_2^*}$  tend to the stable cycle  $C_2$ .

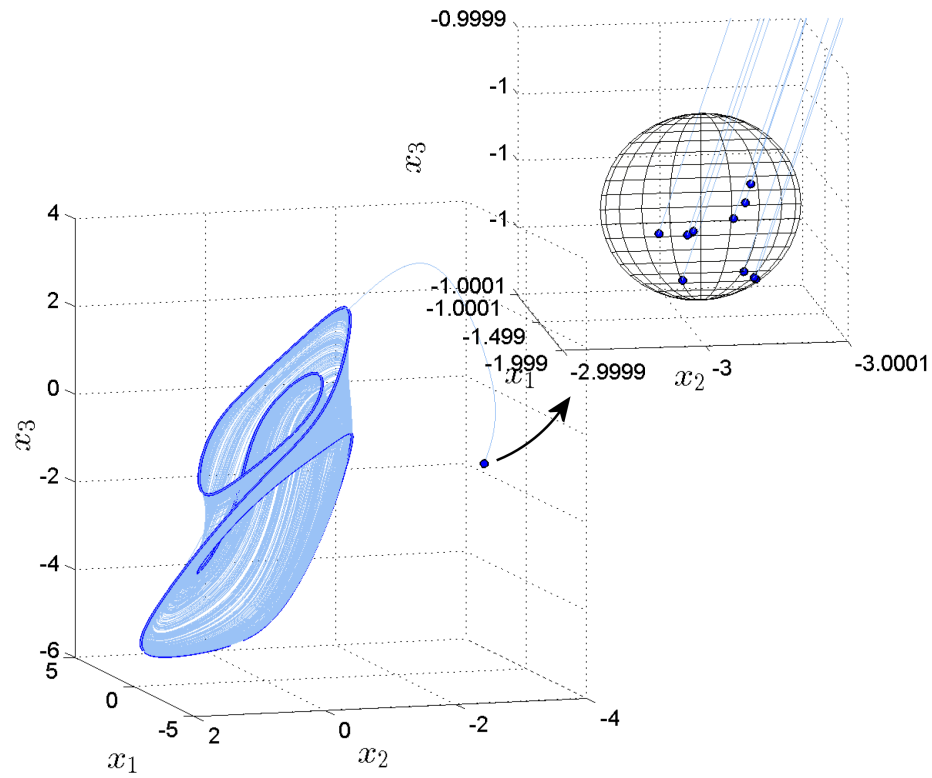


Figure 5: Ten trajectories starting from neighborhoods of  $(-1.9, -3, -1)$ .

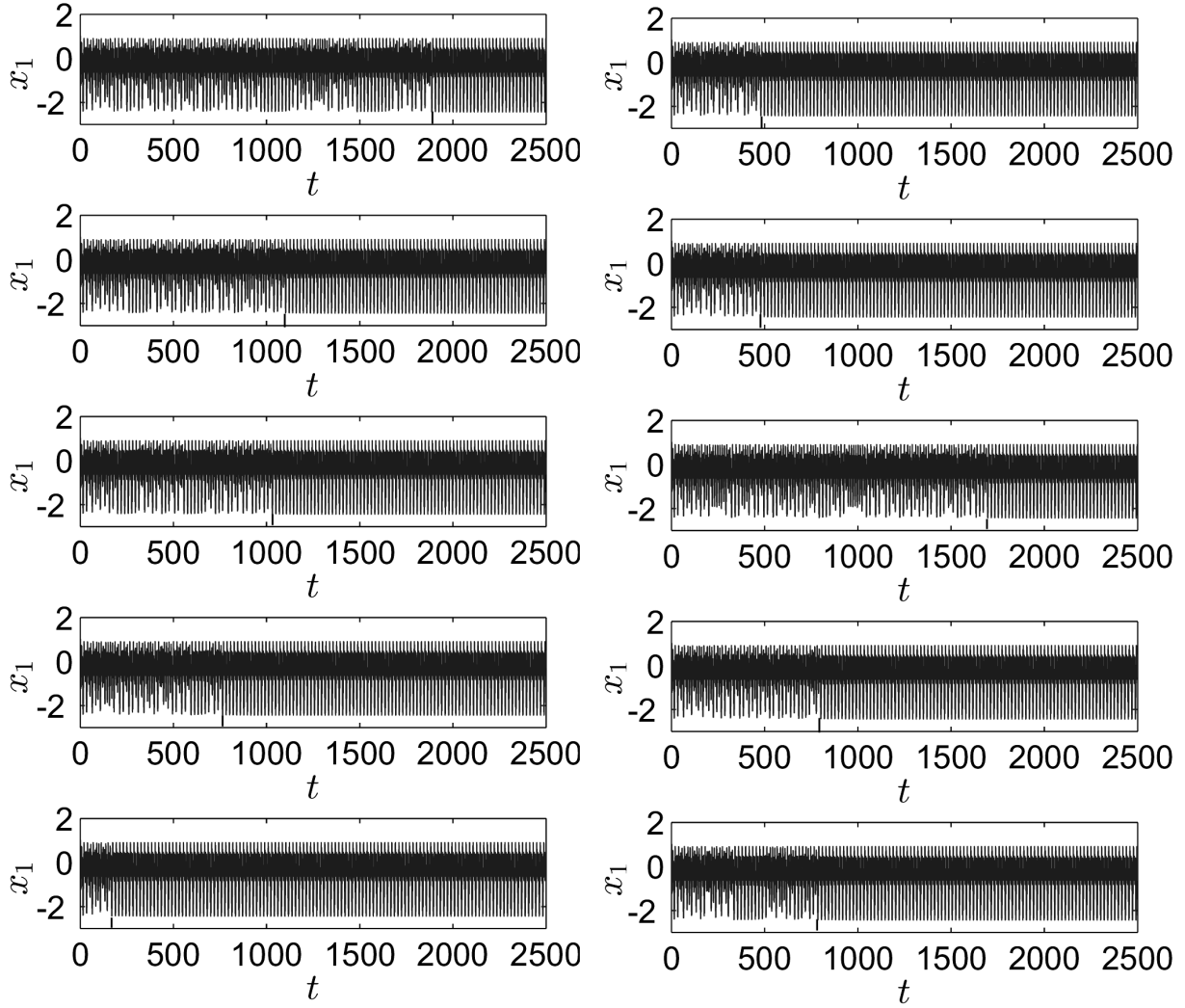


Figure 6: Time series of the trajectories in Fig. 5 starting from the neighborhood of  $(-1.9, -3, -1)$ .

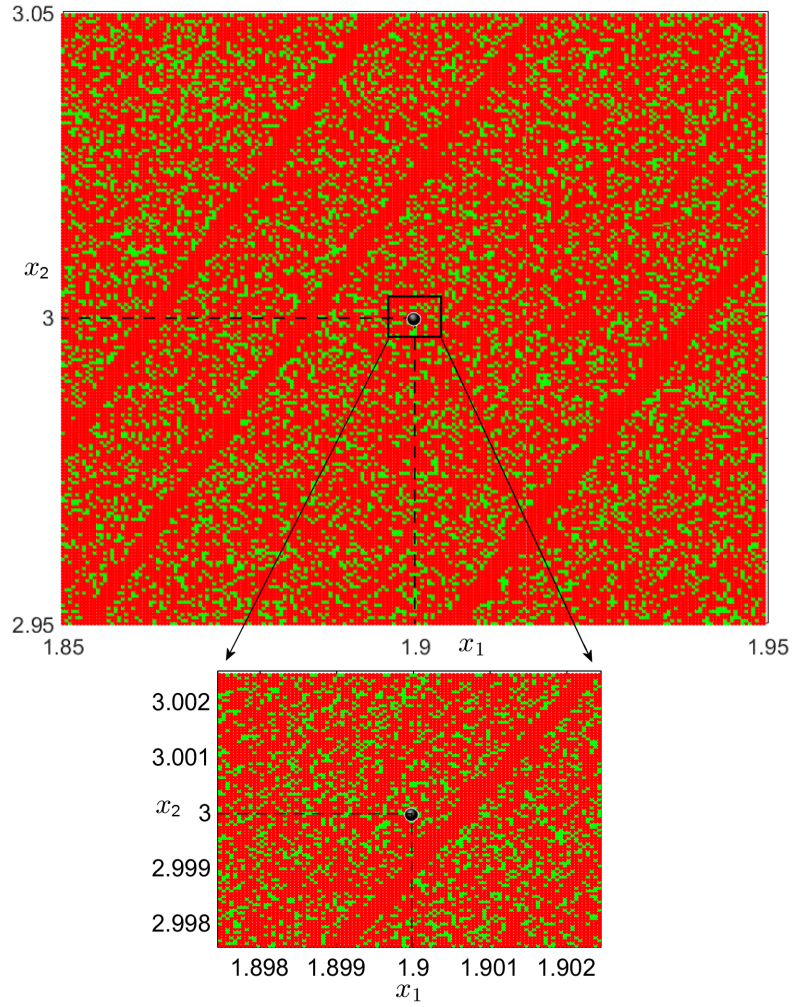


Figure 7: Fractal attraction basin of the hidden chaotic transient  $H_1$  (green) and of the stable cycle  $C_1$  (red). The zoomed region reveals the selfsimilarity. Both regions are centered on  $(1.9, 3)$ .

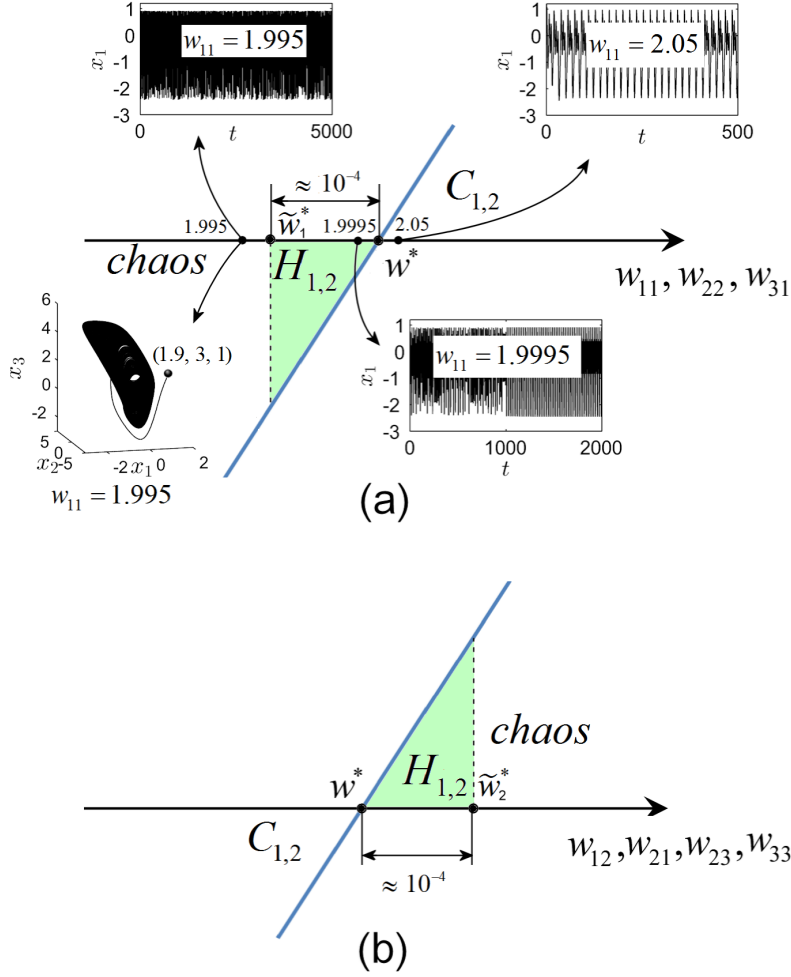


Figure 8: Dynamics of the HNN (2) subject to parameters variations (sketch). a) Variations of parameters  $w_{11}, w_{22}, w_{31}$ . For  $w_{11}, w_{22}, w_{31} < \tilde{w}_1^*$  the system presents hidden chaotic attractors; for  $\tilde{w}_1^* < w_{11}, w_{22}, w_{31} < w^*$ , the system presents hidden chaotic transients (green area), while for  $w_{11}, w_{22}, w_{31} > w^*$  the system evolves along one stable cycle. The considered cases represent the three different dynamics corresponding to three different parameter ranges for the case of the parameter  $w_{11}$  perturbed around  $w^* = 2$  and with the rest of the parameters fixed; b) Variations of parameters  $w_{12}, w_{21}, w_{23}, w_{33}$ . For  $w_{11}, w_{22}, w_{31} < w^*$  the system evolves along one stable cycle; for  $w^* < w_{11}, w_{22}, w_{31} < \tilde{w}_2^*$ , the system presents hidden chaotic transients (green area), while for  $w_{11}, w_{22}, w_{31} > \tilde{w}_2^*$  the system presents hidden chaotic attractors.